Available online at www.sciencedirect.com
ScienceDirect
Chemical Physics 350 (2008) 69–74
Chemical Physics
www.elsevier.com/locate/chemphys

Auger recombination dynamics in Hg_{13}^- clusters

Graham B. Griffin [a], Aster Kammrath [a], Oli T. Ehrler [a], Ryan M. Young [a], Ori Cheshnovsky [b], Daniel M. Neumark [a,c,*]

[a] Department of Chemistry, University of California, Berkeley, CA 94720, United States
[b] School of Chemistry, The Raymond and Beverly Sackler Faculty of Exact Sciences, Tel Aviv University, Tel Aviv 69978, Israel
[c] Chemical Sciences Division, Lawrence Berkeley National Laboratories, Berkeley, CA 94720, United States

Received 14 September 2007; accepted 10 December 2007
Available online 21 February 2008

Abstract

Electronic relaxation dynamics following interband excitation from the 6s to the 6p band in mass selected Hg_{13}^- clusters are measured through femtosecond time-resolved photoelectron imaging (TRPEI). This interband transition is pumped at 4.65 eV and probed at 1.55 eV. Auger decay of occurs on a timescale of 490 ± 100 fs, and a similar time constant is seen for the transient excited state population created by the pump pulse. These time constants are an order of magnitude faster than those seen in previous experiments in which the lone p-electron in Hg_{13}^- was excited within the p-band. The results presented here imply that substantial relaxation of either electrons in the p-band or the hole in the s-band takes place prior to Auger emission, with electron–electron scattering playing a key role in the fast observed dynamics.

Keywords: Mercury; Clusters; Time-resolved photoelectron imaging; Photoelectron imaging; Auger; Auger dynamics; Auger recombination; Electron relaxation dynamics; Excited state relaxation dynamics; Electronic excited state relaxation

1. Introduction

A primary goal of cluster science is to understand how the properties of matter evolve with size and, in particular, to determine how large a cluster has to be before it begins exhibiting properties characteristic of the corresponding bulk material [1]. Metal clusters are especially interesting in this regard, as their study reveals how electronic structure evolves from the discrete states of a single atom or small molecule towards the delocalized bands of the solid [2,3]. Photoelectron spectroscopy (PES) of mass selected metal cluster anions has served as an excellent means of monitoring this evolution, as it directly yields the electronic energy levels of the neutral cluster generated by photodetachment [4–7]. Complementary time-resolved PES experiments explore how the dynamics of electronic excitation in metal cluster anions depend on both size and elemental composition [8–11]. In this paper we report time-resolved photoelectron imaging experiments on Hg_{13}^-, expanding on previous photoelectron experiments on mercury cluster anions [12–16], and establish, for the first time, the timescale for Auger decay dynamics in mercury cluster anions.

In divalent metal clusters (i.e. Groups II and XII) the closed-shell $s^{2n}p^0$ valence electronic structure causes small clusters to be insulators while at some larger size the cluster must evolve to the metallic electronic structure of the bulk metal. Mercury clusters have been extensively studied by both the experimental [17–19] and theoretical [20–22] communities as an example of such divalent metal systems. At small sizes, neutral mercury clusters are bound by van der Waals forces, the dimer being bound by only 47 meV [23]. Autoionization [24] and PES [25] experiments on neutral Hg_n clusters have demonstrated a transition from van der Waals to covalent bonding in the $13 \leqslant n \leqslant 20$ size range,

* Corresponding author. Address: Department of Chemistry, University of California, Berkeley, CA 94720, United States.
E-mail address: dneumark@berkeley.edu (D.M. Neumark).

0301-0104/$ - see front matter © 2007 Elsevier B.V. All rights reserved.
doi:10.1016/j.chemphys.2007.12.005

an interpretation consistent with theoretical work [26]. At larger cluster sizes, the transition from covalent bonding to a metallic electronic structure occurs when the 6s and 6p bands merge. Busani et al. [12] measured the evolution of this band gap via PES of Hg_n^- ($n = 3$–250) anion clusters, which have a lone p-electron. They predicted by extrapolation that the bands would merge completely at $n = 400 \pm 50$, at which point the Hg_n cluster would have metallic electronic structure. In a more recent PES experiment with a tunable laser source, Busani et al. [13] excited the s → p electronic transition in Hg_n^- and saw evidence for electron emission driven by Auger decay following charge carrier thermalization.

These one-photon PES experiments motivated time-resolved photoelectron imaging experiments aimed at following the relaxation dynamics in Hg_n^- clusters subsequent to electronic excitation [14,15]. In these experiments, the lone p-band electron in cluster anions ranging in size from 7 to 18 atoms was excited at one of two pump energies, 1.57 or 1.0 eV, and found to relax back to the bottom of the p-band on time-scales of 2–30 ps, depending on both cluster size and pump photon energy. These dynamics were interpreted as a "cascade" of sequential radiationless transitions through the p-band of the Hg_n^- cluster, eventually leaving the cluster vibrationally hot but in its electronic ground state. Kinetic modeling using a master equation approach and a uniform density of states (DOS) in the p-band reproduced the primary features of the experimentally observed excited state dynamics.

In this paper, we use a higher pump energy ($h\nu_{pump} = 4.65$ eV) to monitor relaxation dynamics following interband excitation of an electron from the s-band of Hg_{13}^- into the p-band. In contrast to our earlier time-resolved experiments, the initially prepared state now has two electrons, rather than one, in the p-band. As a result, the time-scale for electron emission via Auger decay can be determined. The considerably faster dynamics observed here, in comparison to our earlier experiments on relaxation of a single p-electron, provide insight into correlated electron dynamics in the p-band.

2. Experiment

The experiment has been described previously [27,28] and only a brief overview is presented here. Hg_n^- clusters are generated by expanding ~30 psig of Ar with the vapor pressure of Hg at 220–240 °C through an Even–Lavie pulsed solenoid valve [29] equipped with a pulsed ionizer that generates ions via secondary electron attachment, with both the valve and the ionizer operated at 50–100 Hz. Anions are then perpendicularly extracted into a Wiley–McLaren type time of flight mass spectrometer [30], and the anion of interest is isolated using an electrostatic switch. The resolution of the mass spectrometer at the size range of interest is sufficient to separate Hg_n^- from adjacent cluster sizes but not to resolve isotopes for a given value of n.

Femtosecond laser pulses are generated using a commercial Ti:Sapphire oscillator/regenerative amplifier system (Clark-MXR NJA-5/CPA-1000). Under typical operating conditions, the system generates 80–100 fs pulses around 800 nm (1.55 eV) with ~900 μJ/pulse at 500 Hz. In this experiment, the third harmonic of the fundamental at 4.65 eV serves as the pump pulse (~25 μJ/pulse) while the 1.55 eV fundamental is used as the probe pulse (~90 μJ/pulse). The probe pulse is delayed relative to the pump by means of a retro-reflector set on a computer-controlled translation stage, and the beams are then recombined and focused at the interaction region by a 1 m focal length lens.

Photoelectrons are projected by collinear velocity map imaging (VMI) onto a dual micro-channel plate coupled to a phosphor screen [31]. A charge-coupled device camera then collects the images for analysis, typically collected for ~50,000 laser shots total, with ~1–10 photoelectrons collected per shot. The two dimensional electron kinetic energy distributions collected are reconverted into 3-dimensional distributions by an inverse Abel transform using the BASEX method [32] and photoelectron spectra are generated by angular integration of the center ($\phi = 0$) slice of the distribution, with the typical energy resolution ($\Delta E/E$) being ~5%.

3. Results

Fig. 1 shows one-color photoelectron spectra of Hg_{13}^- taken with photon energies of 1.55 eV (a) and 4.65 eV (b). Fig. 1a shows one sharp feature A centered at an electron kinetic energy (eKE) of 1.25 eV. In Fig. 1b, we observe three features: B, a sharp feature that peaks at 2.84 eV, E, a considerably broader feature on the low eKE side of B, and F, for which the onset is around 0.6 eV.

Time-resolved PE spectra are shown in Fig. 2, a waterfall plot of the photoelectron spectra at varying delay between pump and probe laser pulses at photon energies of 4.65 and 1.55 eV, respectively. In order to account for variations in ion intensity, the PE spectra at each delay have been normalized to the total photoelectron count of background scans performed at regular intervals throughout the experiment. Features A, B, E, and F appear at the same eKE values as the corresponding features in the pump-only and probe-only PE spectra. A, B, and F all show changes in intensity only near zero delay while retaining constant intensity in the negative delay and positive delay regions. E exhibits complex dynamics, decreasing in intensity slightly near $t = 0$ and then increasing at later times; this behavior is most clearly seen in Fig. 3, which shows the results of gated integration over selected energy ranges to illustrate several time-dependent features of interest; these energy ranges are listed in the figure caption. Finally, a new feature, labeled G, appears near zero delay. G is broad and does not display an identifiable peak. It appears near time zero and decays with increasing time delay.

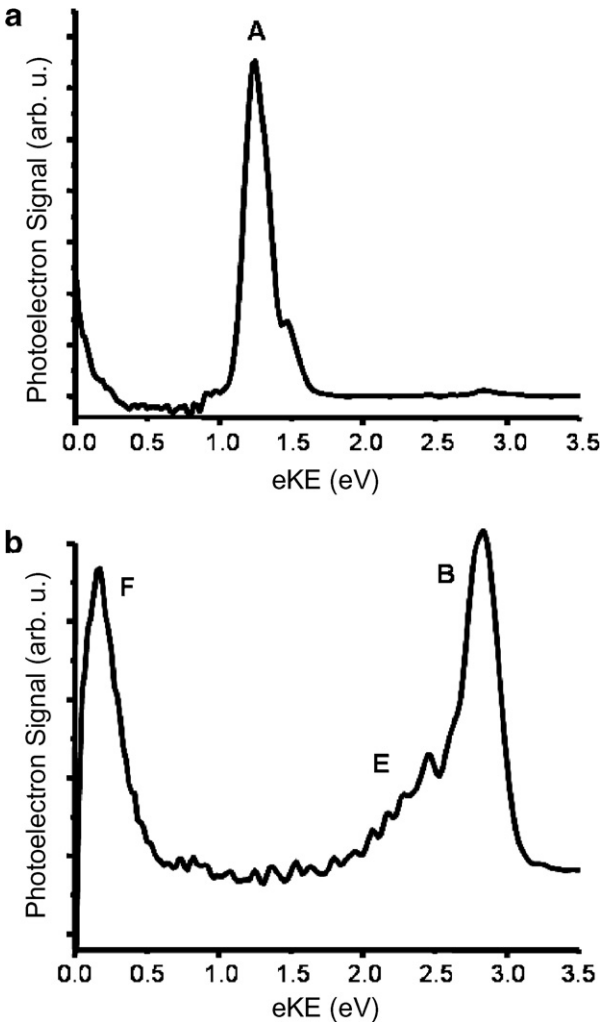

Fig. 1. One-color photoelectron spectra of Hg_{13}^- taken at 1.55 eV (a) and 4.65 eV (b).

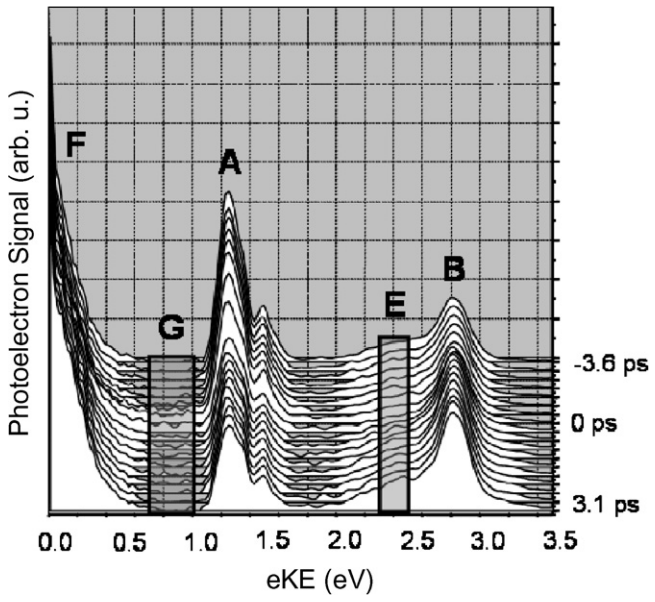

Fig. 2. Waterfall plot of two color photoelectron spectra of Hg_{13}^- taken with $h\nu_{pump} = 4.65$ eV and $h\nu_{probe} = 1.55$ eV. Delay increases from back to front, and features are labeled with reference to Fig. 1 and Section 3.

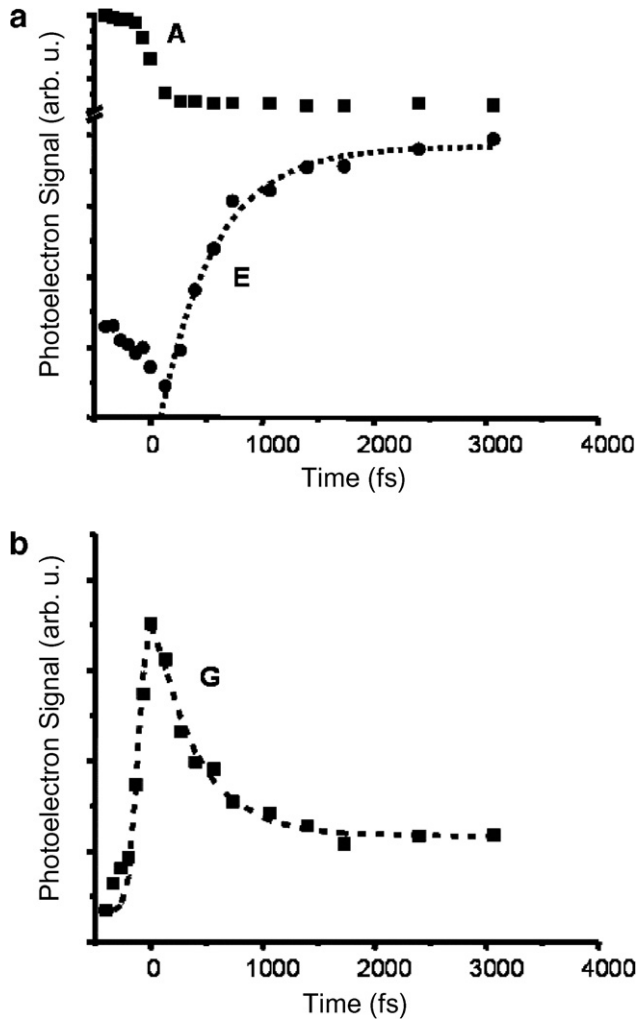

Fig. 3. (a) Auger electron signal integrated from 2.34–2.54 eV eKE (circles, feature E) along with the associated exponential growth fit line (dotted line) and the intensity of 2 photon detachment from the p-band with $h\nu = 1.55$ eV integrated from 1.12–1.32 eV (squares, feature A). (b) Intensity of $[1 + 1']$ photoelectron signal integrated from 0.71–1.02 eV eKE (squares, feature G) along with the fit line discussed in Section 4 (dotted line).

The features in Figs. 1 and 2, many of which have been seen previously [12–15], can be assigned with reference to Fig. 4. The energetics in Fig. 4 are specific to Hg_{13}^-; the bottom of the p-band and top of the s-band lie 1.81 and 4.08 eV below the vacuum level, as determined by previous photoelectron spectra of Hg_{13}^- [12,14]. Feature A in Fig. 1a is from resonant two-photon detachment of the lone 6p electron. Significant photoelectron intensity is also apparent near zero electron kinetic energy (eKE), most likely due to thermionic emission as discussed in our previous work [14]. In Fig. 1b, features B and F are from one-photon detachment from the p- and s-bands, respectively. Feature E, analogous to previous observations by Busani et al. [13], is from the Auger decay process in Fig. 4. Here, the pump photon excites an s-electron to the p-band, producing an excited electron in the p-band in addition to the electron already at the bottom of the band. The excited

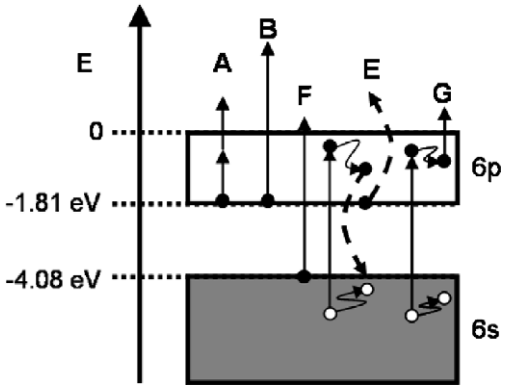

Fig. 4. Diagram describing and labeling the energetics and dynamical processes observed in Hg_{13}^-. The labels here correspond to those used in other figures and in discussion. Filled circles represent electrons while empty circles represent holes. Straight arrows indicate excitation by either 1.55 eV (short arrows) or 4.65 eV (long arrows) photons. Curved arrows indicate dynamical change in binding energy and dashed arrows indicate electron/hole recombination with associated secondary electron ejection.

electron and corresponding s-band hole relax prior to recombining, and the energy released by recombination, which is less than the pump photon energy, ejects the other p-electron. Feature G is the only feature that appears solely in the time-resolved spectra. As discussed below, it appears to be from the transient p-band electron created by the pump laser pulse.

4. Analysis and discussion

In this section, we focus on the time-dependence of the features in Fig. 2 and the interpretation of the underlying dynamics. As shown in Fig. 3, the intensity of feature A (squares, top panel) drops quickly near time zero. This change is cross-correlation limited ($\omega_{cc} \approx 175$ fs, fwhm) and reflects depletion effects resulting from the reversal of the order in which the laser pulses arrive. At positive delay, the pump pulse at 4.65 eV has depleted the anion population via direct detachment from the p-band before the 1.55 eV probe pulse arrives. Feature B (not shown) exhibits the opposite effect, namely a cross-correlated rise around time zero; here the probe pulse depletes the anion population at negative delay before the pump pulse arrives. Neither of these time-dependent trends stem from cluster dynamics.

In contrast, features E and G exhibit time–evolution well beyond the cross-correlation of the pump and probe pulses. Feature E drops near $t = 0$ and then gains intensity with a fitted time constant of $\tau_E = 490 \pm 100$ fs, while feature G rises abruptly at $t = 0$ and falls off exponentially with time constant $\tau_G = 390 \pm 100$ fs, which is indistinguishable from τ_E within the error bars of the two fits. The opposite intensity behavior but similar time constants observed for the two features suggest that they represent complementary probes of the same dynamical phenomena.

The time-resolved dynamics of feature E, assigned to the Auger emission signal, can be understood as follows. At large positive time delays, feature E is produced by absorption of a single pump photon followed by Auger decay, as in Fig. 1b. At large negative time delays, the Auger signal is less intense because the anion population is depleted by two-probe photon detachment of the lone 6p electron prior to arrival of the pump pulse. Near $t = 0$, when the pump and probe pulses start to overlap, the Auger signal is depleted further, indicating that in this time regime the probe pulse detaches the excited p-electron created by the pump pulse before relaxation and Auger emission can occur. Such a process must be more efficient than depletion of the anion population at large negative time delays, else feature E would rise, not fall, near $t = 0$. In fact, as shown below, this second depletion mechanism involves absorption of one probe photon, not two as is required at negative time delays. At longer times, the increase in feature E with time constant τ_E directly yields the overall time constant for Auger emission, because with increasing time, the probe pulse can only detach those clusters that have not undergone neutralization via Auger decay.

Our interpretation of the feature E dynamics would suggest that there is transient p-band population created by the pump pulse whose lifetime can be monitored directly in our pump–probe experiment. Feature G appears to be the likely signature of this population since its decay lifetime, τ_G, is close to the overall time constant τ_E for Auger decay. We propose that feature G is created by the pump pulse exciting an electron from the filled 6s band into the 6p band. This electron can be then detached with a single probe photon as long as it remains bound by less than 1.55 eV, as shown in Fig. 4. Once the electron either is bound by more than 1.55 eV or decays by electron–hole recombination, the pump–probe signal in the range of feature G will disappear. While consistent with this assignment, the eKE range over which feature G occurs, 0.71–1.02 eV, further restricts the observed range of binding energies for the excited electron to 0.53–0.84 eV. The eKE range over which this pump–probe signal could occur is significantly larger, but we can only see it clearly over a fairly narrow range because there are large one-photon features (A and F) on either side of G.

Our results show unambiguously that Auger emission occurs within 400–600 fs of the pump pulse. It is of interest to consider other processes occurring along with Auger emission, because once the electron is excited into the p-band by the pump pulse, multiple relaxation pathways are available. The excited electron can lose energy within the p-band or it can drop back down to the s-band via electron–hole recombination, leading to Auger emission. In addition, since the hole created by the pump laser lies within the 6s band, relaxation within this band can also occur prior to recombination. These processes can in principle occur sequentially or in parallel, complicating efforts to elucidate the detailed dynamics through measurement of what appears to be a single time constant. However,

from previous experimental results, we can place some constraints on the possible dynamical pathways.

First, if electron–hole recombination occurred instantaneously, with no prior relaxation, the energy released would equal the pump photon energy, and the Auger electron would be ejected with the same eKE as from direct detachment with a pump photon (i.e. the eKE of feature B). In fact, as pointed out by Busani et al. [13], the Auger signal is at lower eKE than the direct detachment signal, indicating that some thermalization of the electron and/or hole occurs prior to Auger emission. Second, the transient electron signal, feature G, shows no evidence for shifting in energy with time; this would be a clear signature of electronic relaxation within the p-band. However, it is possible that some shift in the binding energy of the excited electron does occur and is not observed due to low signal level or overlap with higher intensity features F and A. In addition, because initial excitation is possible over a range of energies within the broad s-band, the clusters are likely excited to a range of initial excited states. This would obscure any change in binding energy of the initially excited states. In either case, as stated above, relaxation must take place before Auger electron ejection and must occur within the p-band, the s-band or both simultaneously.

We have previously measured time constants of 6.6 and 4.7 ps for relaxation of the lone 6p electron in Hg_{13}^- excited at 1.5 and 1.0 eV [14,15]. These time constants were interpreted in terms of a series of radiationless transitions in which electronic energy within the p-band is converted into vibrational energy of the cluster. The dynamics observed in the current experiments are an order of magnitude faster than those previously observed for Hg_{13}^-. However, in the current experiments there are two electrons in the p-band instead of just one, allowing for electron–electron interactions that could result in considerably faster relaxation of the initially excited electron within the p-band. Electron–electron scattering from electrons in closely spaced molecular orbitals has been invoked to explain the sub-ps dynamics seen in transition metal clusters [8,9,33] and metal nanoparticles [34]. Thus, scattering between the two p-band electrons in this experiment could allow for faster conversion of electronic energy into vibrational energy within the cluster.

Relaxation could also occur within the 6s band subsequent to hole formation by the pump pulse. The pump pulse at 4.65 eV can, in principle, create a hole over a fairly wide energy range within the 6s band, ranging from 0.57 to 2.27 eV below the top of this band; these values correspond to excitation of an electron to the detachment threshold of the cluster and bottom of the 6p band, respectively. If the hole relaxed to or near the top of the 6s band much faster than 400–600 fs, then recombination followed by Auger emission would produce a broad band, as seen experimentally, without requiring any accompanying shifts in feature G. Alternatively, rapid delocalization of the s-band hole could lead to a Hg_2^+ core within the cluster, by a mechanism similar to that proposed for formation of He_2^+ when He clusters are ionized [35]. In either case, the observed time constants τ_E and τ_G reflect the excited state lifetime with respect to recombination and Auger emission, without requiring prior relaxation within the p-band.

Currently we cannot determine if relaxation occurs predominantly in the s- or p-band, and it is certainly possible that relaxation in both bands occurs. According to both experiment and theory [17,19,24,26], Hg_{13} lies in the transitional size range between van der Waals and covalent bonding in mercury clusters, so studies of the type performed here on slightly larger and smaller clusters will provide a clearer picture of the possible relaxation scenarios in these species. Such studies are currently in progress in our laboratory.

5. Conclusions

The dynamics of electronic relaxation following s to p interband excitation of mass selected Hg_{13}^- anion clusters have been measured. Auger decay of the excited clusters was found to occur on a timescale of 490 ± 100 fs. This timescale is also an upper limit on the rate of transfer of energy from electronic to vibrational degrees of freedom, and is an order of magnitude faster than results previously reported on such electronic relaxation in Hg_n^-. This difference is interpreted as the result of correlated electron dynamics, and mechanisms are posited for relaxation of both the excited electrons in the p-band and the hole in the s-band.

Acknowledgments

This research is supported by the National Science Foundation under Grant No. DMR-0139064. Additional support is provided by the United States–Israel Binational Science Foundation (BSF), Jerusalem, Israel, Grants 2000-333 and 2004-401. O.T.E. is grateful to the A. von Humboldt Foundation (Germany) for the award of a Feodor-Lynen fellowship.

References

[1] A.W. Castleman Jr., K.H. Bowen Jr., J. Phys. Chem. 100 (1996) 12911.
[2] B. Issendorff, O. Cheshnovsky, Annu. Rev. Phys. Chem. 56 (2005) 549.
[3] R.L. Johnston, Philos. Trans. Roy. Soc. London A 356 (1998) 211.
[4] D.G. Leopold, J. Ho, W.C. Lineberger, J. Chem. Phys. 86 (1987) 1715.
[5] O. Cheshnovsky, K.J. Taylor, J. Conceicao, R.E. Smalley, Phys. Rev. Lett. 64 (1990) 1785.
[6] H. Handschuh, C.-Y. Cha, H. Moller, P.S. Bechthold, G. Gantefor, W. Eberhardt, Chem. Phys. Lett. 227 (1994) 496.
[7] H. Wu, S. Desai, L.-S. Wang, Phys. Rev. Lett. 77 (1996) 2436.
[8] N. Pontius, P.S. Bechthold, M. Neeb, W. Eberhardt, Phys. Rev. Lett. 84 (2000) 1132.
[9] N. Pontius, G. Luttgens, P.S. Bechthold, M. Neeb, W. Eberhardt, J. Chem. Phys. 115 (2001) 10479.

[10] M. Niemietz, P. Gerhardt, G. Gantefor, Y.D. Kim, Chem. Phys. Lett. 380 (2003) 99.
[11] P. Gerhardt, M. Niemietz, Y.D. Kim, G. Gantefor, Chem. Phys. Lett. 382 (2003) 454.
[12] R. Busani, M. Folkers, O. Cheshnovsky, Phys. Rev. Lett. 81 (1998) 3836.
[13] R. Busani, R. Giniger, T. Hippler, O. Cheshnovsky, Phys. Rev. Lett. 90 (2003) 083401.
[14] J.R.R. Verlet, A.E. Bragg, A. Kammrath, O. Cheshnovsky, D.M. Neumark, J. Chem. Phys. 121 (2004) 10015.
[15] A.E. Bragg, J.R.R. Verlet, A. Kammrath, O. Cheshnovsky, D.M. Neumark, J. Chem. Phys. 122 (2005) 054314.
[16] R. Busani, O. Cheshnovsky, J. Phys. Chem. C 111 (2007) 17725.
[17] H. Haberland, H. Kornmeier, H. Langosch, M. Oschwald, G. Tanner, J. Chem. Soc. Faraday Trans. 86 (1990) 2473.
[18] B. Bescos, B. Lang, J. Weiner, V. Weiss, E. Wiedenmann, G. Gerber, Eur. Phys. J. D 9 (1999) 399.
[19] K. Rademann, B. Kaiser, U. Even, F. Hensel, Phys. Rev. Lett. 59 (1987) 2319.
[20] H. Kitamura, Eur. Phys. J. D 43 (2007) 33.
[21] G.E. Moyano, R. Wesedrup, T. Sohnel, P. Schwedtfeger, Phys. Rev. Lett. 89 (2002) 103401.
[22] Y. Wang, H.-J. Flad, M. Dolg, Int. J. Mass. Spectrom. 201 (2000) 197.
[23] A. Zehnacker, M.C. Duval, C. Jouvet, C. Lardeuxdedonder, D. Solgadi, B. Soep, O.B. Dazy, J. Chem. Phys. 86 (1987) 6565.
[24] C. Brechignac, M. Broyer, P. Cahuzac, G. Delacretaz, P. Labastie, J.P. Wolf, L. Woste, Phys. Rev. Lett. 60 (1988) 275.
[25] B. Kaiser, K. Rademann, Phys. Rev. Lett. 69 (1992) 3204.
[26] M.E. Garcia, G.M. Pastor, K.H. Bennemann, Phys. Rev. Lett. 67 (1991) 1142.
[27] A.E. Bragg, R. Wester, A.V. Davis, A. Kammrath, D.M. Neumark, Chem. Phys. Lett. 376 (2003) 767.
[28] A.V. Davis, R. Wester, A.E. Bragg, D.M. Neumark, J. Chem. Phys. 118 (2003) 999.
[29] U. Even, J. Jortner, D. Noy, N. Lavie, C. Cossart-Magos, J. Chem. Phys. 112 (2000) 8608.
[30] W.C. Wiley, I.H. McLaren, Rev. Sci. Instrum. 26 (1955) 1150.
[31] A.T.J.B. Eppink, D.H. Parker, Rev. Sci. Instrum. 68 (1997) 3477.
[32] V. Dribinski, A. Ossadtchi, V.A. Mandelshtam, H. Reisler, Rev. Sci. Instrum. 73 (2002) 6317.
[33] N. Pontius, M. Neeb, W. Eberhardt, G. Luttgens, P.S. Bechthold, Phys. Rev. B 67 (2003) 035425.
[34] C. Voisin, D. Christofilos, N.D. Fatti, F. Vallee, B. Prevel, E. Cottancin, J. Lerme, M. Pellarin, M. Broyer, Phys. Rev. Lett. 85 (2000) 2200.
[35] J. Seong, K.C. Janda, N. Halberstadt, F. Spiegelmann, J. Chem. Phys. 109 (1998) 10873.